

New equations for energy dissipation down a stepped spillway

ABSTRACT

Stepped spillways use their stepping nature to dissipate energy in floodwater. Many researchers investigated the hydraulic and geometric relationships of the stepped spillway with slopes above 26.6° degrees, which resulted in energy dissipation. Few, however, studied stepped spillways with slopes below 26.6° degrees, which resulted in energy dissipation with fewer proposing models that estimated its energy losses. The authors reviewed researchers' publications on horizontal stepped spillways with slopes between $3.4^\circ \leq \theta \leq 26.6^\circ$ conducted in skimming flows in large-size facilities with phase-detection intrusive probes. They obtained data sets from them, which they reanalyzed to develop two new No-energy dissipation models that govern skimming flows over a wide range of operating conditions. The new models generated data compared well with the measured data with high coefficients of correlation between 0.95 and 0.99. All the data agree independent of channel slopes and sensor size. The models are simple, easy to use, and render more accurate results than the existing model.

Keywords: Aerated flow, energy dissipation, chute slope, dam height, stepped spillway, skimming flow.

1. INTRODUCTION

Major damage may occur if the energy of floodwater, especially its kinetic energy, is not dissipated safely. One type of flood release facility is the stepped spillway. Their steps offer significant resistance to flow, which result in energy dissipation. This loss in energy leads to the design of smaller and more economical dissipation structures downstream of the chute. As the discharge down the chute increases, a critical value would be reached, beyond which air would enter into the flow. This phenomenon is known as a two-phase flow or Air-Water flow.

Researchers like Horner (1969); Peyras et al. (1992); Chanson (1995, 2001); Ohtsu & Yasuda (1997); Chamani & Rajaratnam (1999); Boes (2000); Matos (2001); Toombes (2002) in the last decades, experimentally investigated air-water flows on stepped spillways with a dam slope above 26.6° degrees. They provided vast information and guidelines for its design.

Few, however, studied stepped spillways with slopes below 26.6° degrees, which resulted in energy dissipation with fewer proposing models that estimated its energy losses. This result in limited information and guidelines for designers of stepped spillways with slopes below 26.6° . There is also a lack of design rules and publications for stepped spillways; Hence, the need for an additional study on stepped spillways. Thus, the authors conducted a study that resulted in better equations and provided design engineers with the knowledge of the impact of a stepped spillway on energy dissipation performance.

Researchers identified three kinds of flows that occur over a stepped spillway. Such flows include:

a) nappe flow regime, b) transition flow regime, and c) skimming flow regime.

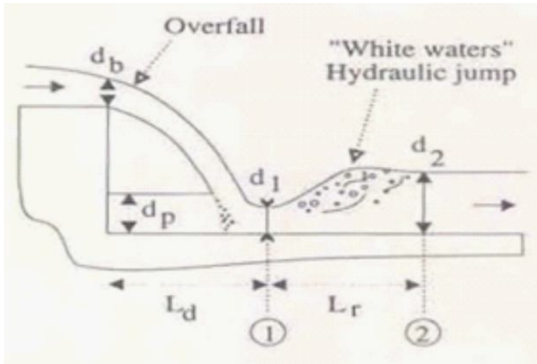
In the nappe flow regime, a sequence of water flows down from one step to the next lower step with the formation of a hydraulic jump at each step. This flow is like a sequence of separate drop structures linked together (Chamani and Rajaratnam, 1994; Chanson, 1993). Energy losses accompany the hydraulic jump. The losses occur due to

a) The disintegration of the spout in the air, and

b) The blending of flow on the steps, with or without the development of hydraulic jump on the step (Chanson, 1994; Rajaratnam, 1990) and these energy losses could be calculated using equations [1.1] or [1.2].

Nappe flow with an established hydraulic jump (Figure 1) usually occurs from small discharges with shallow flow depths. The flow cascades over steps, with the formation of supercritical flow at the edges of the steps, and returns to subcritical flow downstream of the jump.

51 In the nappe flow regime, a sequence of drops from one step to the next lower step occurs with the formation of a
 52 hydraulic jump on each step. This flow type is like a sequence of separate drop structures (Chamani and Rajaratnam
 53 1994; Chanson 1993).
 54
 55



56
 57
 58 **Figure 1: Nappe flow regime (Flow at a drop structure)**
 59

60 The water flows over one step of the spillway to the next lower step with energy loss occurring from: a) the disintegration
 61 of the jet in the air and b) the mixing of the flow on the steps, with or without the development of hydraulic jump, on the
 62 step (Chanson, 1994; Rajaratnam, 1990). The energy losses could be computed using equations [1.1] or [1.2].

$$\frac{\Delta H}{H_o} = 1 - \frac{\frac{d_1}{d_c} + \frac{1}{2} \left(\frac{d_c}{d_1} \right)^2}{H_{max} + \frac{3}{2}} \quad [1.1]$$

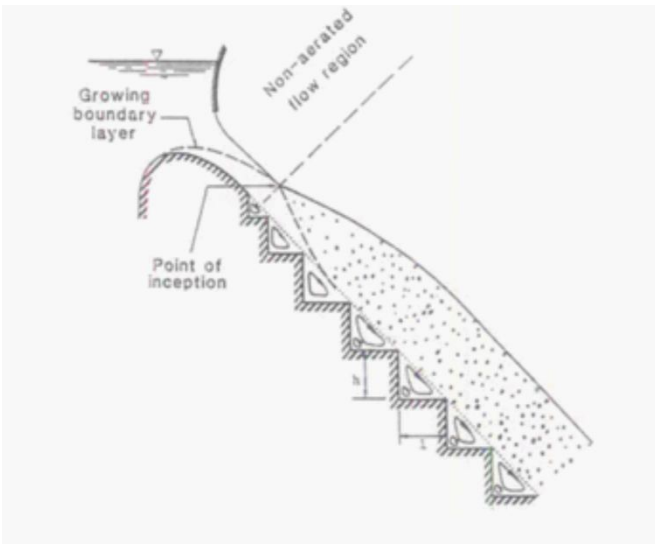
63
 64 Where d_1 is the water depth at impact, d_c is the critical water depth, and H_{max} is the dam height, ΔH is the energy loss, H_o
 65 is the maximum available energy, h is the height of the spillway step. Chanson (1994) later expressed this equation in
 66 terms of the spillway step height, the critical flow depth, and the dam height as:
 67

$$\frac{\Delta H}{H_o} = 1 - \left[\frac{0.54 \left(\frac{d_c}{h} \right)^{0.275} + \frac{3.43}{2} \left(\frac{d_c}{h} \right)^{-0.55}}{\frac{3}{2} + \frac{H_{dam}}{d_c}} \right] \quad [1.2]$$

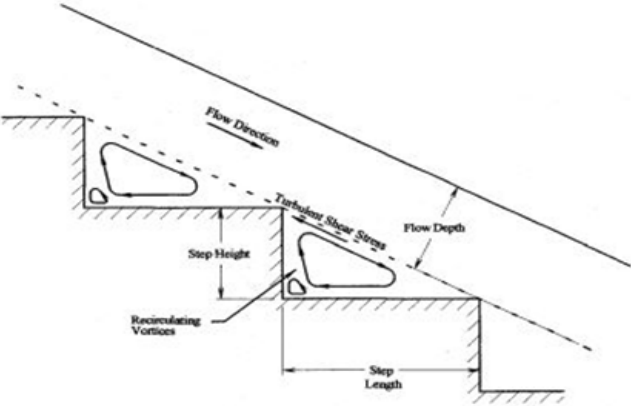
68
 69 Nappe flow with completely established hydraulic jump (Figure 1), usually arises from small discharges with shallow flow
 70 depths and flow over the step with formation of supercritical at the edge of the step and returns to subcritical flow
 71 downstream of the jump.

72 In the skimming flow regime, the flow occurs with the submergence of the steps with the development of a fully aerated
 73 uniform flow downstream of a long chute. Along the upstream steps, a non-aerated flow region exists in which a turbulent
 74 boundary layer develops. Air entrainment in the flow begins where the boundary layer intersects the free surface, referred
 75 to as the point of inception. Downstream of the point of inception, the flow continues to aerate and varies gradually in
 76 depth (Figure 2). The flow eventually becomes a fully aerated uniform flow in which the water depth, velocity, and air
 77 concentration become constant (Bindo et. al 1993) (Figure 3). If uniform flow conditions are reached downstream of the
 78 spillway, this energy loss could be computed as follows

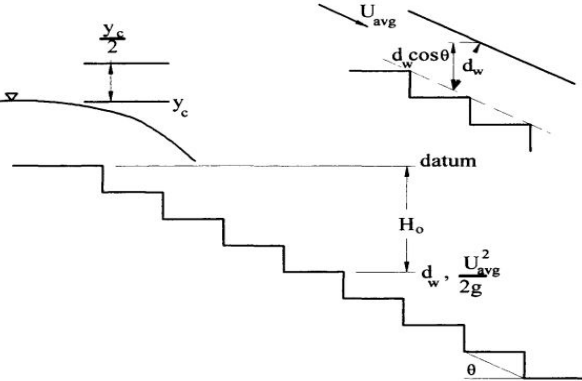
79 In skimming flow, most energy dissipation occurs to keep stable depression vortices.
 80
 81



82
83
84 **Fig. 2. Skimming flow regime - Sorensen (1985)**
85



86
87
88 **Fig. 3. Skimming flow regime with uniform flow conditions**
89



90
91 **Fig. 4. Arrangement of the spillway with the definition of the variables**
92

93 In skimming flow, most of the energy is dissipated in the maintenance of stable depression vortices. If uniform flow
94 conditions are reached at the downstream end of the spillway, this energy loss could be computed as follows
95

$$\frac{\Delta H}{H_{max}} = \frac{d_w \cos \theta + \frac{U_{avg}^2}{2g}}{Nh + \frac{3}{2}d_c} \quad [1.3]$$

Where d_w is the clear water depth, U_{avg} is the average velocity, the total head loss may be rewritten in terms of the friction factor, f , the spillway slope, θ , in degree, the critical depth, d_c , and the dam height, H_{dam} :

$$\frac{\Delta H}{H_{max}} = 1 - \frac{\left(\frac{f}{8\sin\theta}\right)^{1/3} \cos\theta + \frac{E}{2}\left(\frac{f}{8\sin\theta}\right)^{-2/3}}{\frac{H_{dam}}{d_c} + \frac{3}{2}} \quad [1.4]$$

Eq [1.4] was computed for spillway slope with $\theta = 52$ (degrees) and friction factor, $f = 0.03$ and $f = 1.30$, that represent average flow resistance on smooth spillways and stepped spillways, respectively. where E is the kinetic energy correction coefficient, θ is the dam slope in degrees.

2. MATERIALS AND METHODS

The authors carefully selected from the literature 11 No publications on horizontal stepped spillways with minimum step heights of 3 cm, undistorted Froude values and large dimensionless discharges corresponding to Reynolds numbers between 1×10^5 and 1×10^6 (Table 1)

These researchers used experimental facilities on large scale to minimize scale effects that affect the air-water flow processes in high-velocity free-surface flows [15]. Scale effect is defined as slight misrepresentations, which occurs when secondary forces like viscous forces and surface tension forces in turbulent flow are ignored. They are usually overlooked in many open-channel flows. However, if they are ignored in highly air-entrained flows in stepped spillways, where they play significant roles, they could lead to scale effects and to wrong interpretations of results.

Boes (2000), Chanson (2002), Boes and Hager (2003a), and Takahashi et al. (2005) have published works on the impact of scale effects in modelling stepped spillways. Scale effects in stepped spillway models are likely to occur with scales lower than 10:1, Reynolds number smaller than 1×10^5 , Weber number smaller than 100, and step heights lesser than 3 cm. They measured air-water flow properties at all step edges downstream of the inception point of air-entrainment with conductivity phase-detection intrusive probes, optical fiber probes. Use of a Dall Tube flow meter, or V-notch for flow rates, Prandtl-Pitot for flow velocities or Point gauge for clear water flow depth to obtain air-water flows properties is not practicable as large quantities of air are entrained at the air-water interface ().

The principle of the conductivity probe is based on the difference between resistivity of air and water, which provides an instantaneous voltage signal. Threshold technique analyze signals - from a single sensor - used to calculate a) the time-averaged local air concentration or void fraction C , b) the number of air-to-water (or water-to-air) voltage changes expressed as bubble count rate F , and c) the air bubble and water droplet chord sizes. For double-tip conductivity probe with longitudinal separation between the two probe sensors, the cross-correlation analysis of the signals leads to the local time-averaged interfacial velocity V . Details about the signal processing techniques can be found in [8] and [13].

The double-tip conductivity probes used had sensor sizes of $\varnothing = 0.13$ mm and 0.25 mm and were sampled for a period of 45s with a frequency of 20 kHz per sensor.

The discharges comprised transition and skimming flow rates $0.035 \leq qw \leq 0.234$ m²/s for the spillways with $\theta = 8.9^\circ$ and $0.02 \leq qw \leq 0.249$ m²/s for $\theta = 26.6^\circ$ comprising Reynolds numbers of $1.4 \times 10^5 \leq Re \leq 9.3 \times 10^5$ and $8.1 \times 10^4 \leq Re \leq 9.9 \times 10^5$ (Table 1).

Table 1 lists the channel slope, the step height h , the channel width W , the flow rate per unit width q_w , the flow rate dc/h with dc the critical flow depth.

Table 1.1: Summary of the 11 No Publications for the flat stepped spillway with chute angle of $3.4^\circ \leq \theta \leq 26.6^\circ$

| Reference | Slope (θ)deg | Step geometry and Flow conditions | Instrumentation | N (No of Step) |
|--------------------------------------|-----------------------|---|---|----------------|
| Carosi and Chanson (2006) | 21.8 | h (cm) = 10 $dc/h = 1.0 - 1.57$ qw (m ² /s) = 0.095-0.18 $Re = 3.8 \times 10^5 - 7.2 \times 10^5$ | Double-tip ($\varnothing=0.25$ mm) 20kHz/45s | 10 |
| Felder and Chanson (2009a) | 21.8 | h (cm) = 5 $dc/h = 1.17 - 3.16$ qw (m ² /s) = 0.059 - 0.10 $Re = 2.4 \times 10^5 - 4.0 \times 10^5$ | Double-tip ($\varnothing=0.25$ mm) 20kHz/45s | 20 |
| Guenther, Felder, and Chanson (2013) | 26.6 | h (cm) = 10 $dc/h = 0.5 - 1.7$ qw (m ² /s) = 0.03 - 0.217 $Re = 1.2 \times 10^5 - 8.7 \times 10^5$ | Double-tip ($\varnothing=0.025$ mm) 20kHz/45s | 10 |
| Toombes and Chanson (2005) | 3.4 | h (cm) = 14.3 $dc/h = 0.61 - 0.92$ | N/A | 10 |

| | | | | |
|-------------------------------------|-------------|--|---|---------------|
| | | $qw (m^2/s) = 0.08 - 0.15$ $Re = 3.2 \times 10^5 - 6.0 \times 10^5$ | | |
| Bung and Schlenkhoff (2009) | 18.4 & 26.6 | $h (cm) = 3 \text{ \& } 6$ $dc/h = 2.65 - 3.58$ $qw (m^2/s) = 0.07 - 0.11$ $Re = 2.8 \times 10^5 - 4.4 \times 10^5$ | N/A | 2.4 m Hdam |
| Chanson and Toombes (2002b) | 3.4 | $h (cm) = 7.15 \text{ \& } 11.3$ $dc/h = 0.61 - 1.85$ $qw (m^2/s) = 0.08 - 0.15$ $Re = 3.2 \times 10^5 - 6.0 \times 10^5$ | Single-tip ($\varnothing=0.35mm$) 5kHz/60s & 180s | 10 & 18 |
| Ohtsu, Yasuda, and Takahashi (2004) | 5.7 & 11.3 | $h (cm) = 0.63 \text{ \& } 5.0$ $dc/h = 1.25 - 14.3$ $qw (m^2/s) = 0.02 - 0.08$ $Re = 0.8 \times 10^5 - 3.2 \times 10^5$ | Single-tip ($\varnothing=0.1mm$) 2kHz/60s | |
| Thorwarth (2008) | 14.6 | $h (cm) = 5 \text{ \& } 10$ $dc/h = 1.27 - 3.55$ $qw (m^2/s) = 0.05 - 0.234$ $Re = 2.0 \times 10^5 - 9.4 \times 10^5$ | Double-tip ($\varnothing=0.13mm$) 30kHz/40s | 26 |
| Chanson and Toombes (2002a) | 15.9 & 21.8 | $h (cm) = 10$ $dc/h = 0.78 - 1.53$ $qw (m^2/s) = 0.069 - 0.188$ $Re = 2.8 \times 10^5 - 7.5 \times 10^5$ | Double-tip ($\varnothing=0.025mm$) 20kHz/20s | 9 |
| Gonzalez (2005) | 15.9 | $h (cm) = 5 \text{ \& } 10$ $dc/h = 0.6 - 3.2$ $qw (m^2/s) = 0.021 - 0.22$ $Re = 5.0 \times 10^5 - 8.8 \times 10^5$ | Double-tip ($\varnothing=0.025mm$) 20kHz/20s | 9 & 18 |
| Bung (2009) | 18.4 & 26.6 | $h (cm) = 3 \text{ \& } 6$ $dc/h = 2.65 - 3.58$ $qw (m^2/s) = 0.07 - 0.11$ $Re = 2.8 \times 10^5 - 4.4 \times 10^5$ | Double-tip ($\varnothing=0.13mm$) 25kHz/25s | 2.4 m Hdam |
| Gonzalez (2005) | 21.8 | $h (cm) = 10$ $dc/h = 1.1 - 1.7$ $qw (m^2/s) = 0.114 - 0.22$ $Re = 4.6 \times 10^5 - 8.8 \times 10^5$ | Double-tip ($\varnothing=0.025mm$) 20kHz/20s | 10 |
| Felder and Chanson (2014) | 8.9 | $h (cm) = 5$ $dc/h = 1.0 - 3.55$ $qw (m^2/s) = 0.035 - 0.234$ $Re = 1.4 \times 10^5 - 9.4 \times 10^5$ | Double-tip ($\varnothing=0.13mm$) 20kHz/45s | 21 |
| Felder and Chanson (2014) | 26.6 | $h (cm) = 5 \text{ \& } 10$ $dc/h = 0.69 - 3.30$ $qw (m^2/s) = 0.02 - 0.227$ $Re = 0.8 \times 10^5 - 9.1 \times 10^5$ | Double-tip ($\varnothing=0.25mm$) 20kHz/45s | 10 & 20 |
| Felder and Chanson (2014) | 26.6 | $h (cm) = 10$ $dc/h = 0.82 - 1.85$ $qw (m^2/s) = 0.073 - 0.249$ $Re = 2.9 \times 10^5 - 1.0 \times 10^6$ | Double-tip ($\varnothing=0.25mm$) 20kHz/45s | 20 |

137
138
139
140
141
142
143
144
145
146

2.1 Formulation of the models

The authors obtained more than 700 data sets from the 11 No researchers (Table 1.). They reanalyzed about 500 with complete data to formulate energy dissipation models that govern transition and skimming flow over a wide range of operating conditions.

In modeling, it is necessary to determine the values of the parameters that can fit the model of the system it shall describe (Agunwamba, 2007). By the least square method, the best fit curve for this study was formulated as a function of the channel slope, the number of steps, the step height, and the critical water depth using multiple regression analysis and expressed here as:

$$\frac{\Delta H}{H_{max}} = \left[\alpha_o \frac{Nh}{y_c} \right]^{\alpha_1} N^{\alpha_2} h^{\alpha_2} \theta^{\alpha_3} \quad [2.1]$$

147 Where

148
149
150
151
152
153
154

$\frac{\Delta H}{H_{max}}$ is the energy loss ratio,
 H_{max} is the maximum available height,
 N is the number of spillway steps,
 h is the height of the spillway steps,
 θ is the spillway channel slope.

155 They used the measured data sets and multiple regression analysis to solve Equation [2.1] which yielded the values of the
 156 constant α_0 along with the coefficients α_1 , α_2 , α_3 , and α_4 , which are then substituted in Equation [2.1] to give the
 157 developed models in 3.1.
 158

159 3. RESULTS AND DISCUSSION

160
161

161 3.1 Developed models for skimming flow regimes.

162
163
164

3.1.1 Eq [3.1] is valid for use when h (cm) is not more than 20, N is not more 20, θ (degrees) is between 26.6° and 21.8° , and d_c/h is between 1.0 and 3.7.

$$\frac{\Delta H}{H_{max}} = \left[0.049 \frac{Nh}{d_c} \right]^{0.353} N^{0.06} h^{0.124} \theta^{-0.157} \quad [3.1]$$

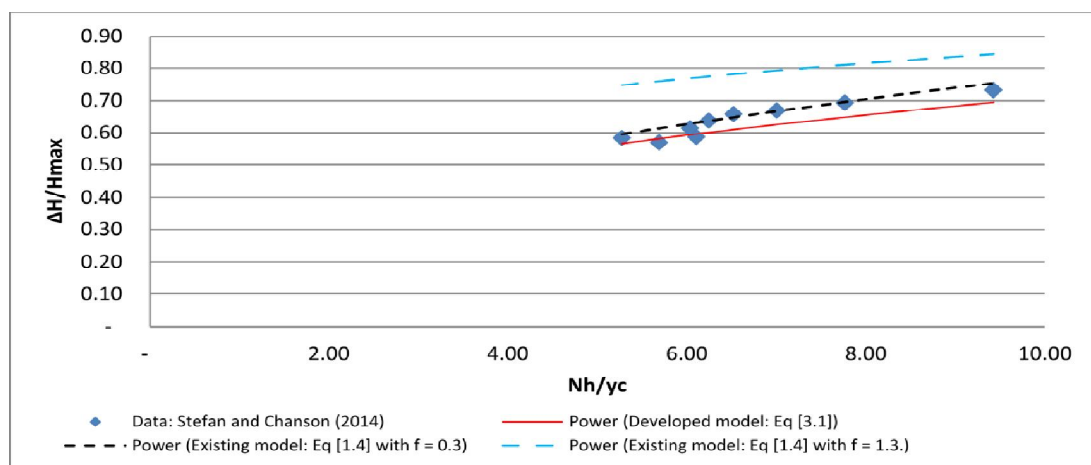
165 **3.1.2** Eq [3.2] is valid for use when h (cm) is not more than 20, N is not more 20, θ (degrees) is between 21.8° and 3.4° ,
 166 and d_c/h is between 1.0 and 3.6.

$$\frac{\Delta H}{H_{max}} = \left[0.029 \frac{Nh}{d_c} \right]^{0.353} N^{0.06} h^{0.124} \theta^{-0.157} \quad [3.2]$$

167
168

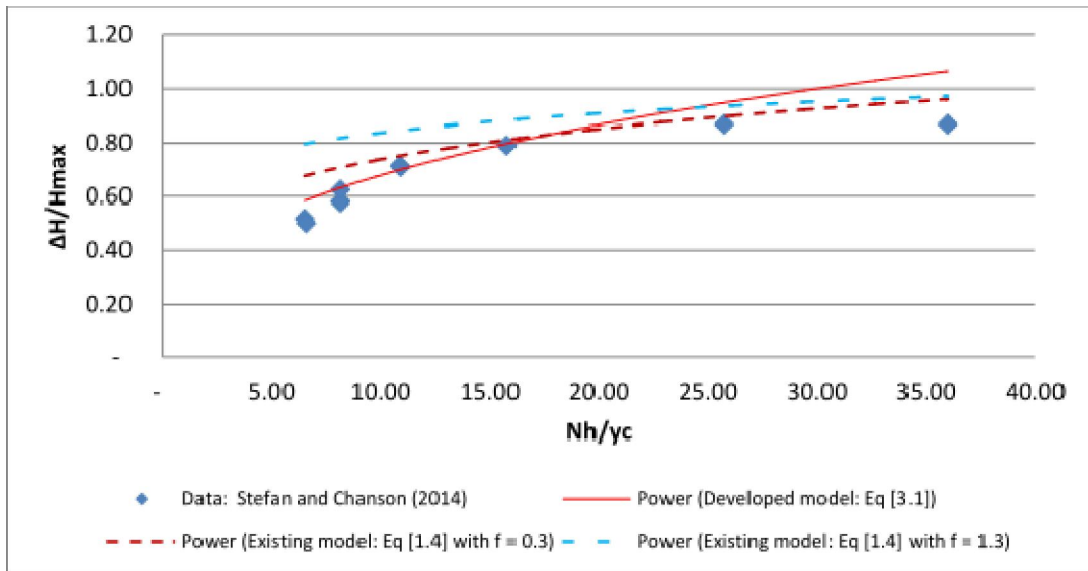
167 3.2. Charts for 3.1.1

169 Figures 5 to 8 depicted the energy loss rates as a function of the expression of a dam height over critical depth for the
 170 measured data, the developed analytical formulation (Eq. [3.1]), the existing model for the computation of energy
 171 dissipation (Eq. [1.4]) with the friction factors of $f = 0.30$ and 1.30 . The figures also show some traditional concave shape
 172 distributions for all the plotted four data sets for energy dissipation for all the flow rates. As seen in the charts, energy
 173 losses increased with decreasing discharges and increased with rising spillway height following earlier investigations
 174 (Matos, 2000; Chanson, 2001b; Felder & Chanson, 2009a). The measured data and the developed model data (Eq. [3.1])
 175 are in close agreement with the coefficients of correlation from 0.96 to 0.99. Again, measured data are in close agreement
 176 with the existing model data (Eq. [1.4]) with a friction factor, $f = 0.3$, yielding the coefficients of correlation between 0.92
 177 and 0.95.
 178

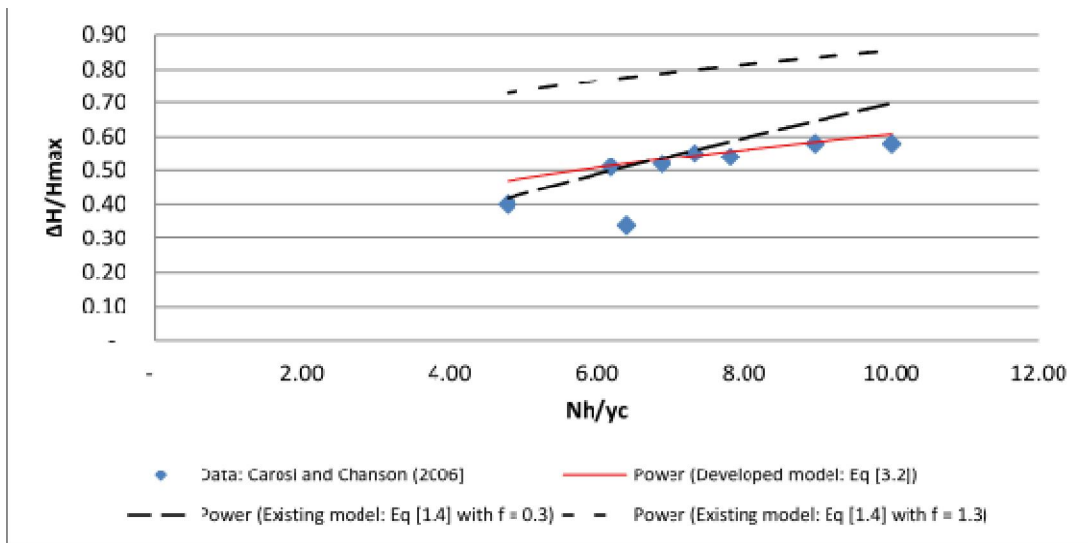


179
180
181
182
183

Fig. 5. $\Delta H/H_{max}$ as a function of Nh/d_c for $\theta = 26.6$, $N = 10$, $h = 10$, $q_w = (0.073 - 0.249) \text{ m}^2 \text{ s}^{-1}$ & $Re = (2.92 \times 10^5 - 9.96 \times 10^5)$, flow rate d_c/h of $(0.82 - 1.85)$.



184
185
186 **Fig. 6.** $\Delta H/H_{\max}$ as a function of Nh/d_c for $\theta = 26.6$, $N = 20$, $h = 5$, $q_w = (0.020 - 0.227) \text{ m}^2 \text{ s}^{-1}$ & $Re = (8.0 \times 10^4 - 9.08 \times$
187 $10^5)$, flow rate d_c/h , of (0.69 - 3.30).]



189
190
191 **Fig. 7.** $\Delta H/H_{\max}$ as a function of Nh/d_c for $\theta = 21.8$, $N = 10$, $h = 10$, $q_w = (0.095 - 0.180) \text{ m}^2 \text{ s}^{-1}$, $Re = (3.80 \times 10^5 - 7.20 \times$
192 $10^5)$, flow rate, d_c/h , of (1.00 - 1.57).]

184
185
186
187
188

189
190
191
192
193

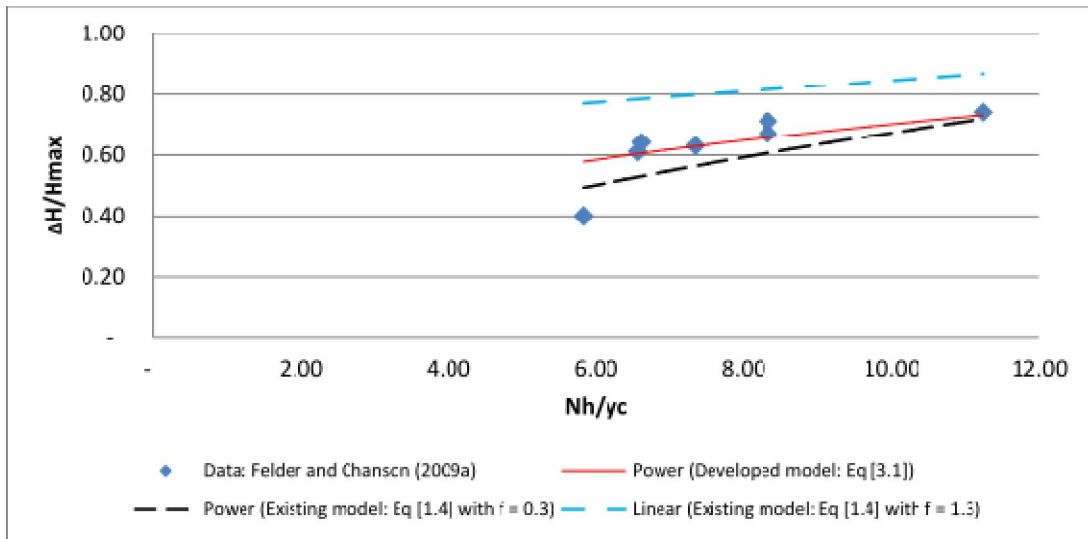


Fig. 8. $\Delta H/H_{max}$ as a function of Nh/d_c for $\theta = 21.8$, $N = 20$, $h = 5$, $q_w = (0.059 - 0.158) \text{ m}^2 \text{ s}^{-1}$, $Re = (2.36 \times 10^5 - 6.32 \times 10^5)$, flow rate, d_o/h , of (0.80 - 1.85).

3.3. Charts for 3.1.2

Figures 9 to 14 depicted energy loss rates as a function of a stepped spillway height over critical depth for the measured data, the developed analytical formulation (Eq. [3.2]), the existing model for the computation of energy dissipation (Eq. [1.4]) with the friction factors of $f = 0.30$ and 1.30 . They displayed similar traditional concave shape distributions for all plotted four data sets for energy dissipation for all flow rates. As shown in the charts, energy losses increase with decreasing discharges and increase with rising dam heights that follow earlier investigations (Matos, 2000; Chanson, 2001b; Felder & Chanson, 2009a). They showed that measured data sets, the developed model data (Eq. [3.2]), and the existing model data (Eq. [1.4]) with friction factor, $f = 0.3$, are in close agreement with the coefficients of correlation from 0.95 to 0.99. Figure 9 showed that the developed model data (Eq [3.2]) was slightly higher than the measured data, increasing with increasing discharges. Figure 10 indicated that the developed model compared well with the measured data than the existing model with $f = 0.10$. Figures 11, 12, and 13 showed that the developed model compared well with field data sets. Figure 14 showed that the developed model predicted values slightly lower than the measured data, while the existing model with $f = 0.10$ produced data sets higher than the field data sets Figure 15 showed an interesting pattern: Rates of energy losses with a stepped spillway slope of 3.4o degrees reduced along the spillway with decreasing discharges and decreased with increasing stepped spillway height. Therefore, the need to investigate why this happened.

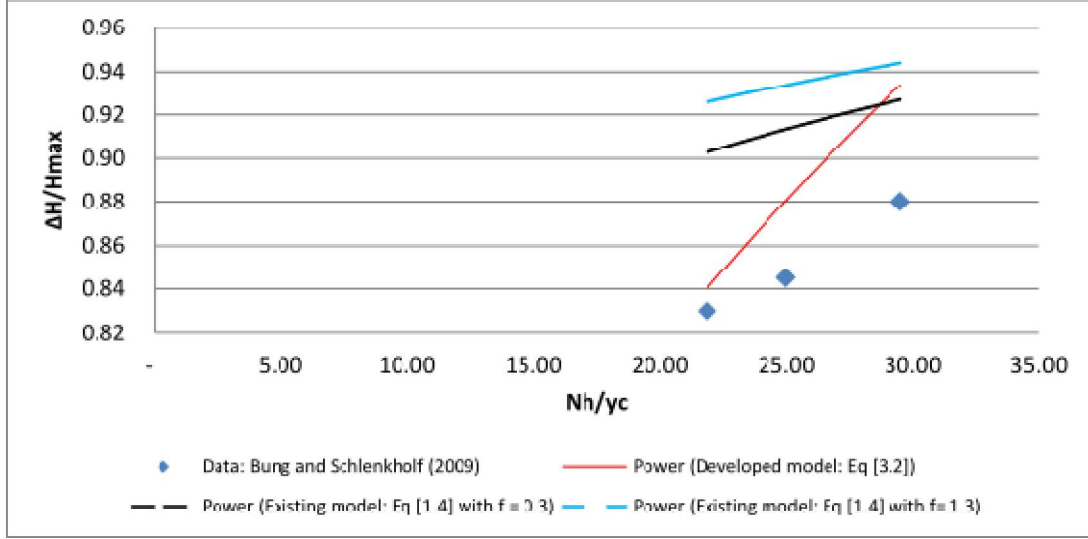
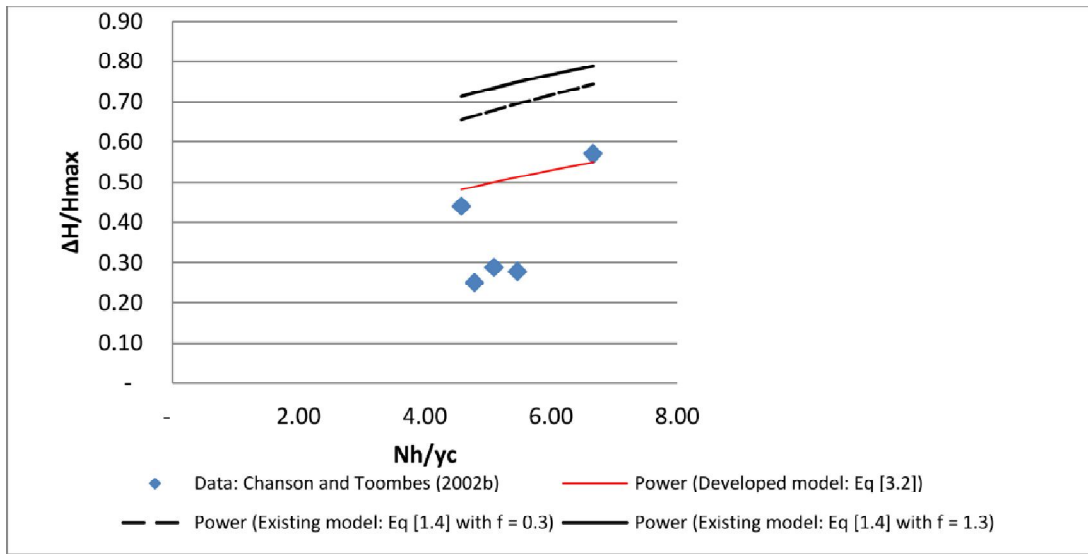
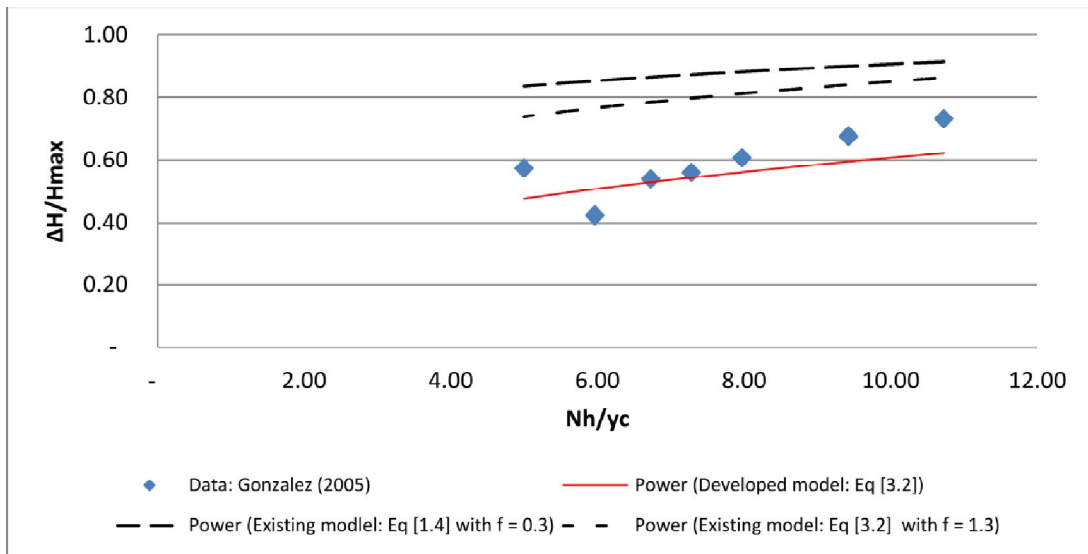


Fig. 9. $\Delta H/H_{max}$ as a function of Nh/d_c for $\theta = 18.4$, $N=40$, $h = 6$, $q_w = (0.059 - 0.158\text{m}) \text{ m}^2 \text{ s}^{-1}$, $Re = (2.36 \times 10^5 - 6.32 \times 10^5)$, flow rate, d_o/h , of (0.80 - 1.85).



220
221
222 **Fig. 10.** $\Delta H/H_{max}$ as a function of Nh/d_c for $\theta = 15.9$, $N = 9$, $h = 10$, $q_w = (0.069 - 0.188) \text{ m}^2 \text{ s}^{-1}$, $Re = (2.76 \times 10^5 - 7.52 \times$
223 $10^5)$, flow rate, dc/h , of (0.78 - 1.53)
224



225
226
227 **Fig. 11.** $\Delta H/H_{max}$ as a function of Nh/d_c for $\theta = 15.9$, $N = 18$, $h = 5$, $q_w = (0.021 - 0.220) \text{ m}^2 \text{ s}^{-1}$, $Re = (8.4 \times 10^3 - 8.8 \times 10^5)$,
228 & flow rate, dc/h of (0.60 - 3.20).
229

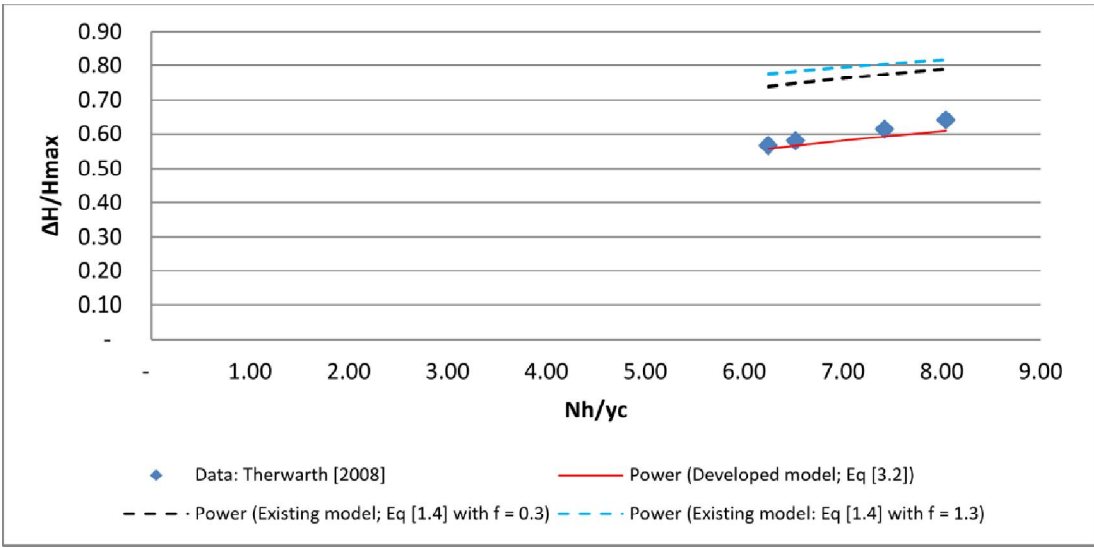


Fig. 12. $\Delta H/H_{\max}$ as a function of Nh/d_c for $\theta = 14.6$, $N = 13$, $h = 10$, $q_w = (0.05 - 0.234) \text{ m}^2 \text{ s}^{-1}$, $Re = (2.0 \times 10^5 - 9.36 \times 10^5)$, & flow rate, d_c/h , of (1.27 - 3.55).

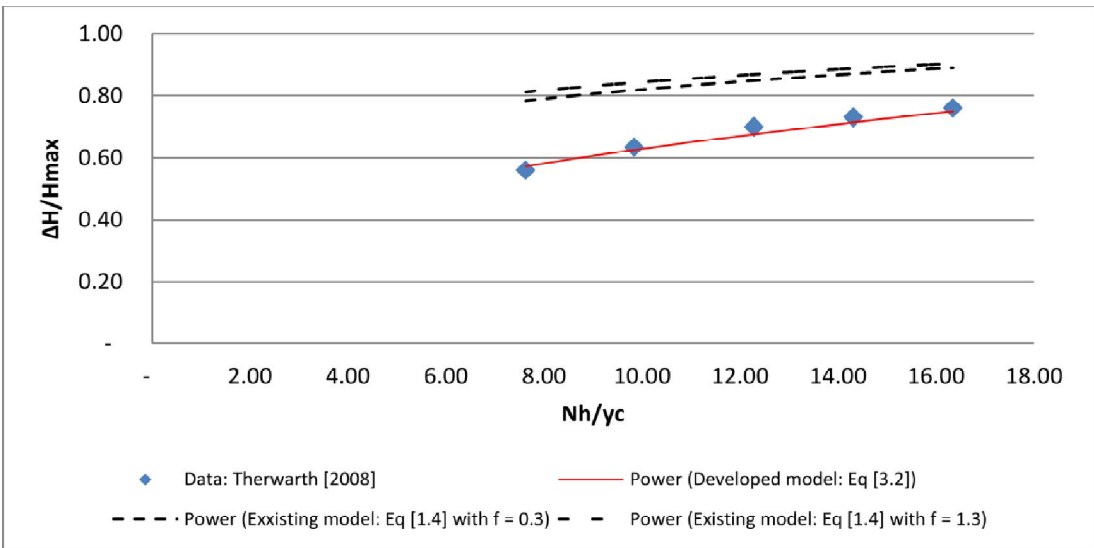
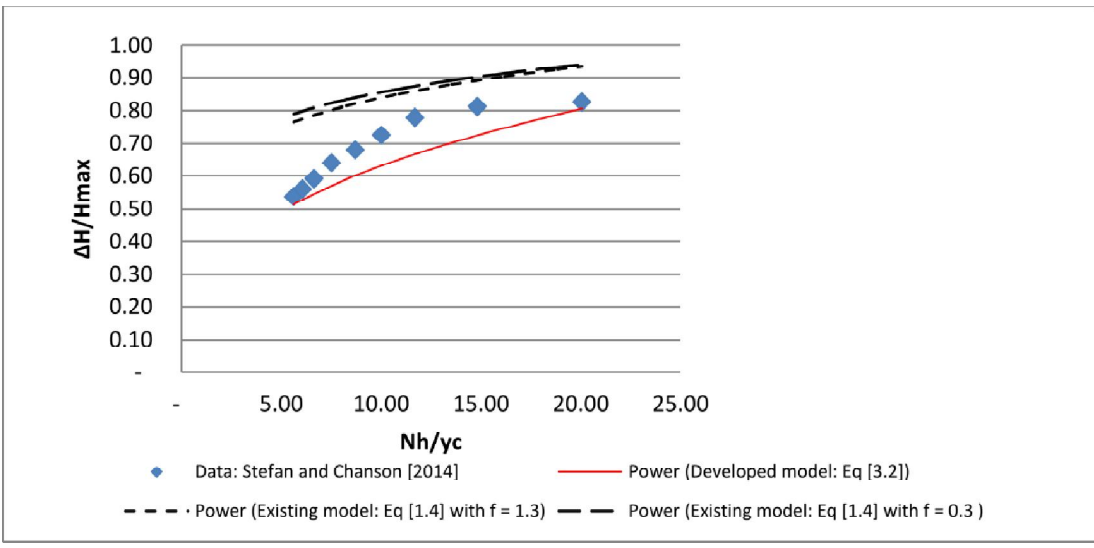


Fig. 13. $\Delta H/H_{\max}$ as a function of Nh/d_c for $\theta = 14.6$, $N = 26$, $h = 10.0$, $q_w = (0.05 - 0.234) \text{ m}^2 \text{ s}^{-1}$, $Re = (2.0 \times 10^5 - 9.36 \times 10^5)$, & flow rate, d_c/h , of (1.27 - 3.55).



230
231
232
233
234

235
236
237
238
239

240

241
242
243
244

Fig. 14. $\Delta H/H_{\max}$ as a function of Nh/d_c for $\theta = 8.9$, $N = 21$, $h = 3$, $q_w = (0.035 - 0.234) \text{ m}^2 \text{ s}^{-1}$, $Re = (1.40 \times 10^5 - 9.36 \times 10^5)$, & flow rate, dc/h , of $(1.0 - 3.55)$.

245
246
247
248
249
250

Fig. 15. $\Delta H/H_{\max}$ as a function of Nh/dc for $q_w = (0.61 - 0.92 \text{ m}^2/\text{s})$, $Re = (2.44 \times 10^6 - 3.68 \times 10^6)$, & flow rate, dc/h , of $0.82 - 1.85$.

4. CONCLUSION

251
252
253
254
255
256
257
258
259

Two new No-models for rates of energy losses in horizontal stepped spillways with slopes below 26.6° degrees, with data based on detailed phase-detection probe measurements, were developed. They generated data compared well with the measured data sets. The new models also produced data sets that were in close agreement with the existing equation for rates of energy losses with friction factor, $f = 0.10$. Rates of energy losses increased along the stepped spillway with decreasing discharges and increased with increasing stepped spillway heights. However, rates of energy losses with a stepped spillway slope of 3.4° degrees reduced along the spillway with decreasing discharges and decreased with increasing stepped spillway height.

260
261
262

ACKNOWLEDGEMENTS

263
264
265

We acknowledge the fruitful discussions with Prof Hubert Chanson of the Department of Civil Engineering, The University of Queensland, Brisbane QLD 4072, Australia.

266
267

COMPETING INTERESTS

268
269

The authors have no competing interests to declare.

270
271

AUTHORS' CONTRIBUTIONS

272
273
274

'Author 1' designed the study, performed the statistical analysis, wrote the protocol, and wrote the first draft of the manuscript. 'Author 2' managed the literature searches. All the authors read and approved the final manuscript.'

275
276

REFERENCES

277
278
279
280
281
282
283

1. Agunwamba J. C (2007), Engineering Mathematical Analysis, pgs 479 – 510, 674 – 675 (ISSN 978-8137-08-3).
2. Boes RM (2000) Zweiphasenströmung und Energieumsetzung an Grosskaskaden, PhD thesis, VAW-ETH, Zürich, Switzerland (in German)
3. Boes, R. M. (2000). Scale effects in modeling two phase stepped spillway flow. In Proc. Intl. Workshop on Hydraulics of Stepped Spillways, 53 - 60. H. E. Minor and W. H. Hager, eds. Steenwijk, the Netherlands: A. A. Balkema.
4. Boes, R. M., and Hager, W. H. (1998). Fiber optical experimentation in two phase cascade flow. In Proc. Intl. RCC Dams Seminar. K. Hanson, ed. Denver, Colo.: Schnabel Engineering.

284 5. Bung DB (2009) Zur selbstbelüfteten Gerinneströmung auf Kaskaden mit gemäßiger Neigung. PhD Thesis, Lehr- und
285 Forschungsgebiet Wasserwirtschaft und Wasserbau, Bergische Universität Wuppertal, Germany (in German)

286 6. Bung DB, Schlenkhoff A (2009) Prediction of oxygen transfer in self-aerated skimming flow on embankment stepped
287 spillways, 33rd IAHR World Congress. Vancouver, Canada

288 7. Carosi G, Chanson H (2006) Air-water time and length scales in skimming flow on a stepped spillway. Application to the
289 spray characterisation. Report No. CH59/06, Division of Civil Engineering, The University of Queensland, Brisbane,
290 Australia, July

291 8. Carosi, G. and Chanson, H. (2006). "Air-Water Time and Length Scales in Skimming Flows on a Stepped Spillway.
292 Application to the Spray Characterisation." Report No. CH59/06, Div. of Civil Engineering, The University of Queensland,
293 Brisbane, Australia, July, 142 pages (ISBN 1864998601).

294 9. Chanson H (1997a) Air bubble entrainment in open channels. Flow structure and bubble size distributions. *Int J Multiph*
295 *Flow* 23(1):193–203

296 10. Chanson H (1997b) Measuring air–water interface area in supercritical open channel flow. *Water Res* 31(6):1414–
297 1420

298 11. Chanson H (2001) The hydraulics of stepped chutes and spillways. Balkema, Lisse, p 418

299 12. Chanson H (2002) Air–water flow measurements with intrusive phase-detection probes. Can we improve their
300 interpretation? *J Hydraul Eng ASCE* 128(3):252–255

301 13. Chanson H (2006) Minimum specific energy and critical flow conditions in open channels. *J Irrig Drain Eng ASCE*
302 132(5):498–502

303 14. Chanson H, Carosi G (2007) Advanced post-processing and correlation analyses in high-velocity air– water flows.
304 *Environ Fluid Mech* 7(6):495–508

305 15. Chanson H, Toombes L (2002a) Air–water flows down stepped chutes: turbulence and flow structure observations. *Int*
306 *J Multiph Flow* 28(11):1737–1761

307 16. Chanson H, Toombes L (2002b) Energy dissipation and air entrainment in stepped storm waterway: experimental
308 study. *J Irrig Drain Eng ASCE* 128(5):305–315

309 17. Chanson, H and Toobes L, "Flow Patterns in Nappe Flow Regime Down Low Gradient Stepped Chutes". *Journal of*
310 *Hydraulic Research* No 46, No 1 (2008), pp 4 – 44 @ International Association of Hydraulic Engineering and Research.

311 18. Chanson, H. *Hydraulics of Nappe Flow Regime Above Stepped Chutes And Spillways*

312 19. Chanson, H. (2002). *The Hydraulics of Stepped Chutes and Spillways*. Steenwijk, The Netherlands: A. A. Balkema.

313 20. Chanson, H., and Toombes, L. (2002). Energy dissipation and air entrainment in a stepped storm waterway: An
314 experimental study. *J. Irrig. and Drainage Eng. ASCE* 128(5): 305- 315.

315 21. Chanson, H.(2002) *The Hydraulics of Stepped Chutes and Spillways*. Lisse, the Netherlands: Balkema.

316 22. Chanson, H (2002), *Hydraulics of Stepped Spillways: Current Status*, *Journal of Hydraulic Engineering*, 126(9), 2000,
317 pp. 636-637.

318 22. Chanson, H. (2000). Characteristics of skimming flow over stepped spillways: Discussion. *J. Hydraul. Eng. ASCE*
319 125(4): 862- 865.

320 23. Chanson, H (1997). "Model Study of a Roller Compacted Concrete Stepped Spillway." *Journal of Hydraulic*
321 *Engineering, ASCE*, Vol 123, No 10, pp, 931- 933 (ISSN 0733 – 9429).

322 24. Chanson, H. (1996) "Prediction of the Transition Nappe/Skimming Flow On a Stepped Channel" *Journal of Hydraulic*
323 *Research*, Vol. 34, 1996 No 3.

324 25. Chanson, H (1994), Comparison of energy dissipation between nappe and skimming flow regimes on stepped chutes,
325 *Journal of hydraulic research*, 32 (2), 1994, pp. 213–218.

326 26 Chanson, H. (1994a). Hydraulics of skimming flows over stepped channels and spillways. *IAHR J. Hydraul. Res.* 32(3):
327 445- 460.

328 27. Chanson, H. (1994b). *Hydraulic Design of Stepped Cascades, Channels, Weirs, and Spillways*. Oxford, U.K.:
329 Pergamon.

330 28. Chanson, H (1994), "Hydraulics of Nappe Flow Regime above Stepped Chutes and Spillways" *Aust, Civil Engg*
331 *Tranports*, I, E, Aust, CE 36 (1), 69 -76

332 29. Chanson, H. (1993). "Stepped Spillway Flows and Air Entrainment." *Can. JI of Civil Eng.*, Vol. 20, No. 3, June, pp.
333 422-435 (ISSN 0315-1468). *JOURNAL DE RECHERCHES HYDRAUQUES*, VOL. 34, 1996, 'Vol. 3 Prediction of the
334 transition nappe/skimming flow on a stepped channel

335 30. Chanson, H (1988), "A Study of Air Entrainment and Aeration Devices on a Spillway Model". Ph.D Thesis, Ref 88 – 8,
336 "Department of Civil Engineering University of Canterbury,

337 31. Chow, V. T. (1959). *Open Channel Hydraulics*. Boston, Mass.: McGrawHill.

338 32. Christodoulou, G. C. (1993). Energy dissipation on stepped spillways. *J. Hydraul. Eng. ASCE* 119(5): 644- 655.

339 33. Felder S (2013) Air–water flow properties on stepped spillways for embankment dams: aeration, energy dissipation
340 and turbulence on uniform, non-uniform and pooled stepped chutes. PhD Thesis, The University of Queensland, Australia

341 34. Felder S, Chanson H (2009a) Energy dissipation, flow resistance and gas-liquid interfacial area in skimming flows on
342 moderate-slope stepped spillways. *Environ Fluid Mech* 9(4):427–441

343 35. Felder S, Chanson H (2009b) Turbulence, dynamic similarity and scale effects in high-velocity freesurface flows above
344 a stepped chute. *Exp Fluids* 47(1):1–18

- 345 36. Felder S, Chanson H (2011) Air–water flow properties in step cavity down a stepped chute. Int J Multiphase Flow
 346 37(7):732–745
- 347 37. Felder S, Chanson H (2013) Aeration, flow instabilities, and residual energy on pooled stepped spillways of
 348 embankment dams. J Irrig Drain Eng ASCE 139(10):880–887
- 349 38. Felder, S., and Chanson, H. (2008). Turbulence and turbulent length and time scales in skimming flows on a stepped
 350 spillway: Dynamic similarity, physical
 351 modeling, and scale effects. Queensland, Australia: University of Queensland, Division of Civil Engineering.
- 352 39. Felder, S and Chanson, H.(2012). "Air-Water Flow Measurements in Instationary Free Surface Flows: a Triple
 353 Decomposition Technique." Hydraulic Model Report No. CH85/12, School of Civil Engineering, The University of
 354 Queensland, Brisbane, Australia
- 355 40. Felder, S. and Chanson, H. (2011a). "Air-Water Flow Properties in Step Cavity down a Stepped Chute." International
 356 Journal of Multiphase Flow, Vol.
- 357 41. Felder, S. and Chanson, H. (2011b). "Energy Dissipation down a Stepped Spillway with Non-Uniform Step Heights."
 358 Journal of Hydraulic Engineering, ASCE, Vol. 137, No. 11, pp. 1543- 1548 (DOI 10.1061/(ASCE)HY.1943-7900.0000455).
- 359 42. Felder, S. and Chanson, H. (2009b). "Turbulence, Dynamic Similarity and Scale Effects in High-Velocity Free-Surface
 360 Flows above a Stepped Chute." Experiments in Fluids, Vol. 47, No. 1, pp. 1-18. 2006 World Environ. and Water
 361 Resources Congress, ASCflow in open channels. J Hydraul Div ASCE 84(HY7):1–35 paper 1890
- 362 43. Ferrell RT, Himmelblau DM (1967) Diffusion coefficients of nitrogen and oxygen in water. J Chem Eng Data
 363 12(1):111–115
- 364 44. Gonzalez CA (2005) An experimental study of free-surface aeration on embankment stepped chutes. PhD Thesis,
 365 Department of Civil Engineering, The University of Queensland, Brisbane, Australia
- 366 45. Guenther P, Felder S, Chanson H (2013) Flow aeration, cavity processes and energy dissipation on flat and pooled
 367 stepped spillways for embankments. Environ Fluid Mech 13(5):503–525
- 368 46. Gulliver JS (1990) Introduction to air–water mass transfer. New Zealand. Hydraulic of Nappe Flow Regime Above
 369 Stepped Chute and Spillways
 370 In: Proceedings of 2nd international symposium on gas transfer at water surfaces, air–water mass transfer; ASCE Publ.,
 371 Minneapolis MN, pp 1–7
- 372 47. Kawase Y, Moo-Young M (1992) Correlations for liquid-phase mass transfer coefficients in bubble column reactors
 373 with newtonian and non-newtonian fluids. Can J Chem Eng 70:48–54
- 374 48. Matos J (1999) Air entrainment and energy dissipation on stepped spillways. PhD Thesis, Technical University of
 375 Lisbon, Portugal
- 376 49. Meireles I, Matos J (2009) Skimming flow in the nonaerated region of stepped spillways over embankment dams. J
 377 Hydraul Eng ASCE 135(8):685–689
- 378 50. Ohtsu I, Yasuda Y, Takahashi M (2004) Flow characteristics of skimming flows in stepped channels. J Hydraul Eng
 379 ASCE 130(9):860–869
- 380 51. Straub LG, Anderson AG (1958) Experiments on self-aerated flow in open channels. J Hydraul Div ASCE 84(HY7):1–
 381 35 paper 1890
- 382 52. Thorwarth J (2008) Hydraulisches Verhalten der Treppengerinne mit eingetieften Stufen - Selbstinduzierte
 383 Abflussinstationaritäten und Energiedissipation. PhD Thesis, University of Aachen, Germany (in German)
- 384 53. Toombes L (2002) Experimental study of air–water flow properties on low-gradient stepped cascades. PhD Thesis,
 385 Dept. of Civil Engineering, University of Queensland, Australia
- 386 54. Toombes L, Chanson H (2005) Air–water mass transfer on a stepped waterway. J Environ Eng ASCE 131(10):1377–
 387 1386
- 388 55. Wood I (1983) Uniform region of self-aerated flow. J Hydraulic Eng 109(3):447–461

390 **LISTS OF SYMBOLS**

- 391
- 392 d_c – critical water depth (m);
- 393 h - step height (m),
- 394 H_1 – residual head at the bottom of the spillway (m);
- 395 ΔH – difference between the maximum head and the residual head (m);
- 396 H - total head (m);
- 397 H_{max} - maximum head available (m):
- 398 $H_{max} = H_{dam} + 3/2 * d_c$;
- 399 Q - discharge ($m^2 s^{-1}$);
- 400 q_w - discharge per unit width ($m s^{-1}$);
- 401 Reynolds number defined as : $Re = \rho_w * U_w * D_H / \mu_w$
- 402 U_w - flow velocity (m/s): $U_w = q_w/d$;
- 403 W - channel width (m);
- 404

405 **Subscript**

406 c – conditions at critical height;
407 N– number of step;
408
409
410
411